Doping carbon electrodes with sulfur achieves reversible sodium ion storage

Perspectives on design of floating platforms for offshore airborne wind energy systems

A. Bertozzi
Faculty of Mechanical Engineering, Delft University of Technology, The Netherlands

F. Niosi & B. Paduano
Dipartimento di Ingegneria Meccanica e Aerospaziale, Politecnico di Torino, Italy

X. Jiang
Faculty of Mechanical Engineering, Delft University of Technology, The Netherlands

ABSTRACT: The need for a fast transition towards electricity generation pushed large investments in high-risk, high-impact technologies such as floating Airborne Wind Energy Systems (AWES), which are expected to be highly cost efficient with respect to state-of-the-art offshore wind energy technology. Current research on the matter does not address the design challenge of a tailored floater, necessary to suit at most the unique features of such systems, and foster their industrial and commercial development. The goal of this study is to review the available solutions from traditional floating offshore wind energy systems, and hence to propose a straightforward concept, adapted from current designs, for the deployment of AWESs. Moreover, to provide insights on how the geometrical parameters influence its motion response, a sensitivity study is performed, testing different design solutions against a wave scatter. In view of a cost-effective solution, a spar-like concept, adapted to the specific needs of AWESs, is proposed. The sensitivity analysis suggests the need to adopt aspect ratio larger than 4 to effectively mitigate the pitch response; in addition, heave response emerges as a possible design constraint with large impact on the device's costs.

1 INTRODUCTION

Floating offshore deployment of Airborne Wind Energy Systems (AWESs) is appealing as it promises a drastic cost reduction with respect to traditional floating offshore Horizontal Axis Wind Turbines (HAWTs). The reduction in costs is important to keep the Levelised Cost of Electricity (LCOE) comparable to traditional floating wind energy systems, and therefore, foster the commercial development of this technology. The expected lower costs are due to two interrelated factors. In general, AWESs require less construction material with respect to HAWTs of comparable nominal power, and therefore, they are also lighter. As a consequence, simpler, smaller, lighter, and hence, less expensive floating platforms with respect to floating foundations for HAWTs can be designed for their support.

The rest of the paper is organised as follows. Section 2 provides a summary of airborne wind energy technology, and proposes a floater concept for the deployment of AWESs, after analysing current floating concepts for offshore HAWTs. Section 3 presents the mathematical modelling framework adopted for the investigation, whilst Section 4 introduces the numerical case study and defines the boundaries for a sensitivity analysis, to then discuss its results. Finally, Section 5 draws the conclusions.

2 LITERATURE REVIEW

Within this section a brief overview of floating airborne systems is provided. Please note that, though this study aims to analyse mainly the floating structure, and the associate wave-hull interaction, the wind-generators are briefly analysed and described in order to keep this study reasonably self-contained.

2.1 *Overview on Airborne Wind Energy Systems*

A significant period elapsed since Loyd (1980) published what is considered the foundation for the quantitative analysis of Airborne Wind Energy Systems

(Ahrens et al. 2013). After a period of stagnation, the new millennium brought an acceleration in the research on the matter. In parallel to academia, industry moved the first steps in the development of onshore systems, which can be classified under four main aspects: the way of interacting with the wind, the way to control the flight, the morphology of the aircraft, and the position of the electrical generators, as illustrated in Figure 1. Considering the *electrical generators position*, in a Fly-Gen AWES small wind turbines are installed onboard the aircraft, and the electrical energy is transmitted to the ground via electrical cables integrated into the tether that physically retains the aircraft. In these systems, conversion from wind to electrical power occurs continuously during operation. In Ground-Gen AWESs, the generator is installed on the ground, instead. Electrical energy is generated by harnessing the traction force transmitted through one or multiple tethers mechanically connecting the aircraft to the ground station, and driving the motion of the generator. Such systems are characterised by cyclic power production.

Concerning the *interaction with the wind*, the majority of the developed concepts rely on crosswind motion. That is, the wing has a prevalent relative velocity component lying on a plane normal to the wind flow. As shown by Fagiano & Milanese (2012), crosswind motion provides a potential power that is about 50 times greater than the power that could be extracted solely from the actual wind speed. Therefore, most AWESs under development aim for crosswind motion.

In terms of *control strategies*, three main architectures are observed: while some systems utilise onboard actuators to move control surfaces, similarly to conventional airplanes, other airborne systems can be equipped with an airborne control pod (*i.e.* the actuators are attached to the flying structure in a control box) attached some meters below the aircraft, controlling the flight dynamics by adjusting the length of the bridles. Finally, some aircraft can also be controlled by adjusting the length of the power ropes, or utilising dedicated control bridles, directly from the ground.

Lastly, AWESs can be classified according to the type of *aircraft* utilised. Ground-Gen systems employ both soft kites and rigid wings, whereas Fly-Gen systems typically use rigid wings exclusively; the interested reader is referred to Cherubini et al. (2015) for a detailed overview of such systems. However, in a general perspective, different type of kites can be used. Although rigid wings systems represent a interesting scenario in terms of aerodynamic performances and lifetime, the associated weight and cost can move towards the use of a fabric kite, aiming to minimise the device cost of energy.

2.1.1 *AWESs for floating offshore deployment*

While in the previous Section a brief discussion and classification of the airborne systems is provided, within this Section we aim to move towards the offshore field, trying to find advantages and disadvantages of the available solution for such novel applications. State-of-the-art of offshore deployment tends to favor the adaptation of a soft kite Ground-Gen concept to floating installations, as presented in Cherubini et al. (2016), Cherubini et al. (2018), and Trombini et al. (2024). This preference is driven by several factors, such as limited clutters of the ground station of such systems, lower costs for the airborne component with respect to rigid wings, high levels of control authority and autonomy demonstrated during experimental flights, and ultimately, relatively large power production exhibited by current prototypes of this kind.

In fact, most Ground-Gen systems currently in operation or close to commercial release, *i.e.* SkySails PN-14 (SkySails Power) or KitePower Falcon (KitePower), are designed with ground stations that can fit into a standard 30 ft container and weight approximately 20 tons. This compact size makes them suitable for installation on small and cost-efficient floaters. In addition, soft kites allow vertical deployment and retrieval of the airborne components, further minimising the space required on the floater.

In terms of power production, rigid wings appear to offer the most efficient solution due to their higher power extraction per wing area. However, besides the higher production costs for this kind of wing, the scalability of these systems has not been proved yet completely: whilst SkySails proved to have the technology to control soft kites up to 320 m^2 for naval traction (Erhard & Strauch 2013), there is no evidence of test flights for medium/large surface area rigid wing systems. For these reasons, research activities in the field of offshore deployment of AWESs lean towards soft wing systems.

Installation of actuators in a pod connected to the kite by control bridles, see Fritz (2013), Erhard & Strauch (2018), van der Vlugt et al. (2013), among others, and to the ground station by a single tether should be preferred, as it appears more robust against disturbances arising from platform's motions. Taking into account the reasons above, for the preliminary design of a floater, a kite pumping generator similar to the SkySails PN-14 has been chosen as given condition for the description of the airborne component.

2.1.2 *Working principle and features of a pumping kite generator*

A pumping kite generator operates on a power cycle defined by two phases: a traction phase, and a return phase. During the traction phase, the main tether is unwound from the winch, driving the motion of the generator, and the kite flies ∞-shaped trajectories in crosswind motion. During the return (passive) phase, the kite is steered to a low power zone, while the electrical machine operates as motor and quickly reels-in the tether so that a new cycle may start. The trajectory

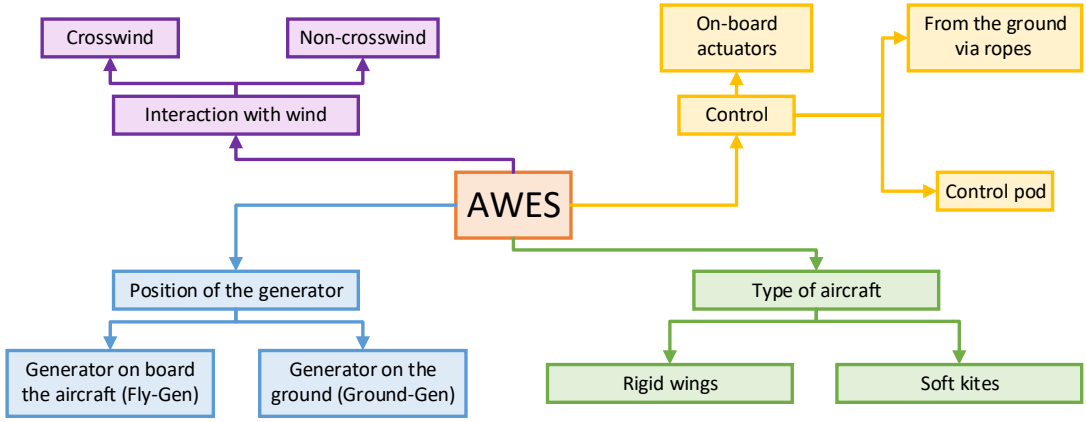

Figure 1: Schematic classification of AWESs according to wind interaction, aircraft type, control strategy, and generator position.

of the kite during an entire power cycle, obtained by post-processing of data from Fagiano et al. (2022), is depicted in Figure 2.

The worst load condition for the floater is observed during the traction phase. To maximise the force during traction, the kite is steered to fly with low elevation angles, ranging from about $25°$ to $45°$. The load has therefore both a horizontal and a vertical component throughout the whole traction phase, unlike the load from traditional HAWTs, in which the vertical component of the load is significantly less influential compared to the horizontal one. Azimuth angles typically range between $-22.5°$ and $22.5°$, symmetrically about the wind direction (Fagiano et al. 2022). The maximum force is observed for minimum elevation and null azimuth. An advantageous aspect of this

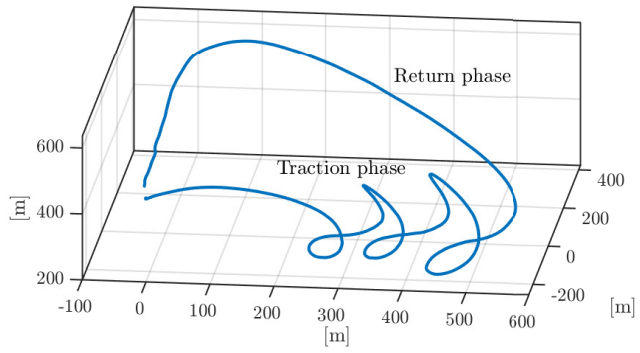

Figure 2: Experimental kite trajectory during a power cycle.

loading condition is related to the associated point of application. In the bi-dimensional case, on the longitudinal plane XZ, depicted in Figure 3, the distance d between the application point P of the aerodynamic load $\vec{\boldsymbol{F}}$ and the rotation point R of the platform (around the Y-axis, normal to the plane) is relatively small. This results in minimal overturning moments on the floater caused by the aerodynamic loads, unlike traditional HAWTs.

Please note that aerodynamic modelling of the pumping kite generator and coupled aero-hydrodynamic analysis of the overall systems are outside the scope of this work. Nevertheless, the unique characteristics of the aerodynamic load should be qualitatively taken into account in the preliminary design of the floater and of the mooring system.

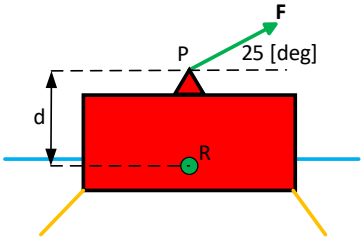

Figure 3: Application of aerodynamic load on floating offshore AWESs.

2.2 *Floating structures for offshore systems*

The initial step in defining the design of a floater for offshore deployment of AWESs in deep water environment involves exploring existing design solutions developed to tackle similar challenges. This includes examining platforms designed for offshore deployment of traditional wind energy systems, which have evolved over time to meet specific technological needs (Edwards et al. 2024). Similarly, AWES platforms are expected to undergo a similar design evolution. Current designs for such structures utilise various physical principles to fulfill their function, which yield specific advantages and disadvantages for each design. Figure 4 depicts some of the most common concepts observed in both research and industry. Accordingly, we aim to start by briefly analysing such structures trying to outline their features in a pro and cons fashion. Analysing floaters, the primary types used for HAWTs include the spar, the tension leg platform, the barge, the semi-submersible, and the HexaFloat.

Spar buoys, depicted in Figure 4a, are essentially tall, slender cylindrical columns, with ballast situated in the bottom part to ensure the center of mass is as

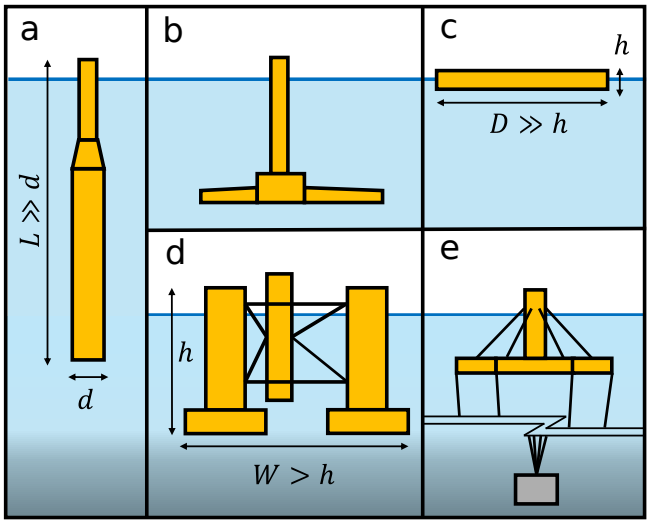

Figure 4: Floater concepts for floating offshore HAWTs: (a) spar, (b) tension leg platform, (c) barge, (d) semi-submersible, (e) HexaFloat.

close to the base as possible. Stability is achieved by leveraging the restoring moment from the ballast, often in combination with a catenary mooring system (Edwards et al. 2024). Their simple geometry facilitates manufacturing, and their small waterplane area helps to limit heave motions. However, their large draft prevents them from being positioned upright in a harbor, leading to the need for horizontal towing followed by offshore ballasting (Jiang 2021). The considerable length of these structures in the horizontal position poses challenges during towing operations.

Tension Leg Platforms (TLPs), illustrated in Figure 4b, are vertically moored compliant platforms characterised by a central column connected to mooring lines via radially spreading arms. The structure is designed with excess buoyancy to pre-tension the mooring system, providing restoring forces and moments. TLPs may not be self-stable while free-floating during transit and installation, so these systems are often transported on barges or secured to auxiliary buoyancy structures to ensure stability for towing. The need for expensive anchors capable of bearing significant vertical loads due to high mooring pre-tensions contributes to higher overall costs compared to spar and semi-submersible platforms, so that TLPs are less commercialised in the sector (Jiang 2021).

Barges, represented in Figure 4c, utilise a large waterplane area for stabilisation. This is achieved by having a diameter (or equivalent horizontal dimension, in the case of polyhedral structures) that is much larger than their height. This configuration allows to increase the moment of area of the waterplane area, increasing hydrostatic stiffness in roll and pitch (Edwards et al. 2024).

Semi-submersibles, illustrated in Figure 4d, consist of three to five vertical cylindrical columns connected together by slender pontoons. These system are able to achieve stability by leveraging both the large waterplane area and gravity stabilisation. These floaters are normally very large, as increasing the distance between the columns further increases the moment of area of the waterplane area and, therefore, stability in roll and pitch. Circular or hexagonal heave plates are often installed on the lateral columns to dampen heave oscillations. Semi-submersibles are relatively easy to tow, simplifying their installation and decommissioning processes (Jiang 2021). In addition, their large stiffness in pitch and roll can effectively counteract the significant overturning moments given by the large HAWTs planned for the close future. These unique characteristics make semi-submersibles highly desirable, positioning them as the most favored concept at present. While simpler geometric designs are being developed with the aim to minimise the number of slender elements, gradually replacing them with box-shaped pontoons, semi-submersibles still pose challenges in manufacturing compared to spars and TLPs, making them more complex and expensive to produce (Edwards et al. 2024).

The scheme depicted in figure 4e depicts the *HexaFloat*, a relatively recent floater concept developed by Saipem S.p.A. and patented in 2018 (Saipem S.p.A. 2022). This innovative design features a hexagonal-shaped structure with a central column supporting the wind turbine. A counterweight is linked to the hexagonal structure via six tethers, one for each vertex. Depending on the water depth, catenary or taut mooring configurations with three or six lines are proposed. One interesting aspect of this concept is its adaptability to various turbine sizes. Specifically, the ballast mass and depth can be adjusted to accommodate different payload masses, while maintaining similar overall dimensions for the structure regardless of turbine size (Ghigo et al. 2020).

2.2.1 *Proposed floater concept*

As outlined in the preceding Sections, each design has its own advantages and disadvantages, summarised in Table 1. With a primary goal of achieving cost-effectiveness in terms of both material and installation expenses, and taking into account the specific challenges and potentials associated with the aerodynamic loads generated by pumping kite generators, our conceptual design leans towards adapting the spar concept to better suit AWES technology.

As AWES have a smaller mass than HAWTs, the modified spar could be considerably smaller and lighter too, reducing some of the typical disadvantages of traditional spars, correlated to the huge mass and dimensions of such structures (e.g. difficulty in towing out when in horizontal position, very deep water needed). The high sensitivity to pitch and roll can be moderated by adopting a taut mooring system with synthetic lines, which is also necessary to bear the vertical component of the aerodynamic load.

Table 1: Advantages and disadvantages of FOWTs platforms.

Floater type	Pros	Cons
Spar	Easy to manufacture Small heave motions	Hard to tow out Turbine should be installed offshore Heavy and large structure Large pitch and roll Large seabed footprint Small deck Very deep water needed
TLP	Small heave, roll and pitch motions Small seabed footprint Light and small structure	Not self-stable Requires dedicated installation vessel Expensive mooring system Small/no deck
Barge	Easy to tow out Easy to install Large deck Turbine can be installed onshore	Large seabed footprint Large heave motions
Semi-sub	Easy to tow out Easy to install Large deck Turbine can be installed onshore	More difficult to manufacture (w.r.t. spar) Large seabed footprint Large heave motions
Hexafloat (Saipem S.p.A. 2022)	Adaptability to turbine of different sizes Easy to manufacture Small roll and pitch motions Turbine can be installed onshore	Large structure Small deck Very deep water needed Hard installation of the pendulum

3 MATHEMATICAL MODELS

The numerical models adopted for this investigation are detailed and analysed in this section. Note that, in the light of the linearity of the adopted models, a frequency domain approach can be pursued.

3.1 *Frequency domain model*

The equation of motion for a floating device can be written, in the frequency domain, according to the block diagram outlined in Figure 5, as follows:

$$G_d(\omega)q(\omega) = \mathcal{F}_e(\omega) - \mathcal{F}_m(\omega) - \mathcal{F}_a(\omega), \quad (1)$$

$$G_d(\omega) = -\omega^2(M + A(\omega)) + \\ +j\omega(B(\omega) + D) + K, \quad (2)$$

$$\mathcal{F}_m(\omega) = G_m q(\omega), \quad (3)$$

where $q_{eq} \in \mathbb{R}^6$ is the equilibrium position of the moored device, $\{q, \mathcal{F}_e, \mathcal{F}_m\} : \mathbb{R} \to \mathbb{C}^6, \omega \mapsto \{q(\omega), \mathcal{F}_e(\omega), \mathcal{F}_m(\omega)\}$ are the device motions, wave excitation forces, and mooring forces, respectively. Moreover, $\{G_d, G_a\} : \mathbb{R} \to \mathbb{C}^{6\times6}, \omega \mapsto \{G_d(\omega), G_a(\omega)\}$ are the frequency responses relative to device dynamics, and aerodynamic force action, respectively. While in a general, linear, modelling framework, $G_m \in \mathbb{R}^{6\times6}$ represents the mooring restoring matrix, within this study the mooring analysis has been neglected, *i.e.* $G_m = \mathbb{0}^{6\times6}$, being $\mathbb{0}^{n\times m}$, a $n \times m$ null matrix. The device dynamics frequency response G_d can be described in terms of Newton's second law, by defining $\{M, K, D\} \subset \mathbb{R}^{6\times6}$ as the inertia, hydrostatic stiffness, and viscous damping matrices, and $\{A, B\} : \mathbb{R} \to \mathbb{R}^{6\times6}, \omega \mapsto \{A(\omega), B(\omega)\}$ as the added mass and damping frequency dependent matrices. These hydrodynamics properties can be evaluated numerically by leveraging the so-called Ogilvie's function (Ogilvie 1964) by means of a boundary element method (BEM) software, such as OrcaWave, which was selected for this study.

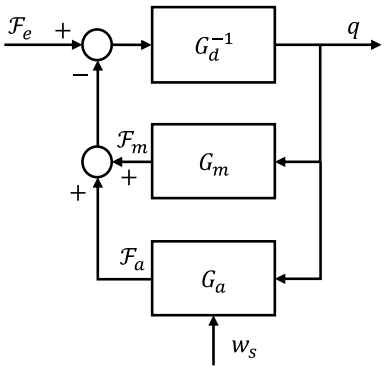

Figure 5: Block diagram of the offshore AWES dynamics

Please note that, in a general perspective, a floating airborne system can be represented as linear time invariant system as schematically represented in Figure 5, in which the mutual interaction of the mooring

system (G_m) and the system aerodynamics (G_a) affects the system response q. Though in general, these systems can not be omitted apriori, within this study we are going to neglect the aerodynamics of the kite, assuming that no significant effect is produced on the device motion, *i.e.* the device (G_d) works as a band-pass filter. Furthermore, being this study based on a preliminary analysis, the results will be definitively conservative, as mooring system is neglected.

4 SENSITIVITY ANALYSIS

4.1 *Definition of the numerical case study*

To gain insights into the influence of the geometrical parameters of the proposed floating assembly on the associated response to environmental loads, we begin by conducting a sensitivity analysis. In particular, among the physical parameters of the floating unit, the external radius and the aspect ratio, defined as the ratio between the external height and the radius, are adopted to conduct the analysis. Furthermore, to maintain a constant free-floating draft to height ratio of $2/3$, as designed for the OC4 semi-submersible (Robertson et al. 2014), the ballast mass is changed accordingly. To ballast the structure marine water ($\rho_w = 1025$ kg/m^3) is used, and the ground station, accommodated inside the floater, is positioned just above the ballast. The cylindrical steel-made shell of the hull ($\rho_{\text{steel}} = 7860$ kg/m^3), is assumed to have a constant thickness of 0.05 m, in line with what proposed in Robertson et al. (2014).

We suppose to install the device close to Pantelleria's island, in Italy, and test different floaters against 16 sea states from the wave scatter depicted in Figure 6, to then weight the results on each sea state respective occurrence. The considered environmental exciting conditions are superposed to the occurrence (top), and energetic (bottom) scatter contours. The ranges for the input parameters, the external radius and the aspect ratio, are bounded from constraints, mostly arising by the need to accommodate the ballast and the ground station inside the cylindrical shell.

Ground station: current research and technical documentation on both onshore and offshore GroundGen AWESs overlooks the detailed design and arrangement for the ground components. The ground station for a 150 kW pumping kite generator is known to fit in a standard 30 ft container, and to have a mass of less than 20 tons. The ground unit of the pumping kite generator comprises of three main components: the winch, the gearbox, and the generator/motor, as illustrated in Figure 7. To account for the additional weight of the structures necessary for fitting the ground station inside the cylindrical shell, and adopting a conservative approach, in this paper the ground station is modelled as a cuboid of dimensions 4.72 m $\times$ 4.72 m $\times$ 2.59 m and having an equivalent density $\rho_{eq} = 346.35$ kg/m^3.

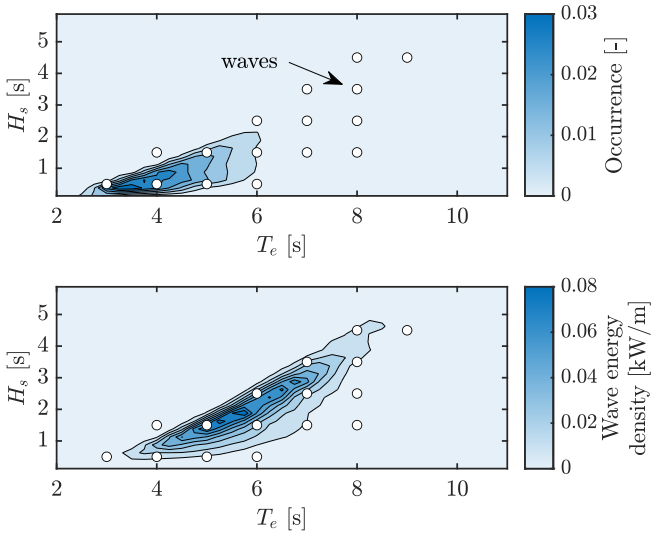

Figure 6: Wave scatter for the Pantelleria site, Italy. Occurrences scatter (top), and energetic scatter (bottom); white markers indicate the waves considered in this study.

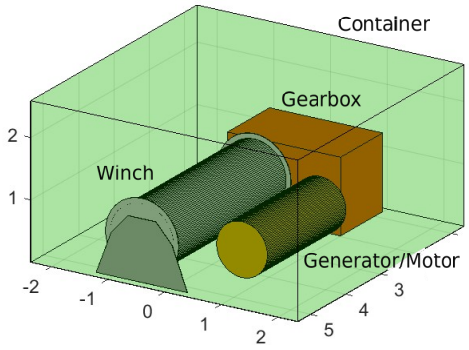

Figure 7: Example of a possible simplified layout for the ground station. The original 30 ft container has been reshaped to a squared prism with equivalent volume for symmetry reasons.

Floater assembly model: once the dimensional constraints stemming from the clutters of the ground station have been defined, ranges for the parameters considered for the sensitivity study can be established. We consider radii varying from 3.5 m to 6 m with a step of 0.5 m, and aspect ratios varying from 2 to 10 with a step of 2. These choices for the parameters yield a total of 30 geometries to be tested. While the lower constraints can be easily imposed by considering, among others, the ground station dimensions, the upper ones are more challenging to be defined a priori; however, within this study, we aim to analyse the general trend of the floater responses given a representatively large set of geometrical parameters.

Floater cost estimation: for each geometry, the corresponding material and construction costs are estimated, assuming a linear cost function with respect to the mass of the hull shell. For all the cases we assume a cost per unit mass of 8.5 €/kg, including supply, fabrication, and assembly costs.

Hydrodynamic analysis: Despite being more computationally efficient than the open source tool Nemoh, thanks to multithreading options, the BEM

software OrcaWave does not have a meshing engine, so that the hull mesh shall be computed externally. Therefore, Nemoh is selected to generate the mesh for each geometry, and the mesh is then imported in OrcaWave for the diffraction analysis. A target number of panel of 500, and 35 angular discretisation steps are set as mesh parameters for all the geometries. A 500 elements linearly spaced frequency vector ranging from 0.01 rad/s to 2.5 rad/s is used for the diffraction analysis. To account for viscous damping, a diagonal external damping matrix has been included in the computation of the displacement response amplitude operators (RAOs), with entries equal to 10% of the critical damping for each degree of freedom.

4.2 *Results*

Within this section, the overall system response is analysed leveraging the non-parametric representation described in Section 3. In details, by means of the linear map G_d^{-1}, the system response can be analysed in the associated spectral characterisation, *i.e.*:

$$S_q = S_\eta G_t G_t^*, \tag{4}$$

where $S_q : \mathbb{R} \to \mathbb{R}^6, \omega \mapsto S_q(\omega)$ represents the device motion spectra and $S_\eta : \mathbb{R} \to \mathbb{R}, \omega \mapsto S_\eta(\omega)$ the wave input spectrum. The map $G_t : \mathbb{R} \to \mathbb{C}^{6\times 6}, \omega \mapsto G_t(\omega)$ represents the wave to motion I/O map, *i.e.* the RAO, given by the combination of the map G_d^{-1} and the so-called excitation coefficients (Journée & Massie 2000), and G_t^* represents the complex conjugate of the map G_t. Given the device motion spectra, the statistical representation of the motion can be defined as the standard deviation $\sigma_{q_i} \in \mathbb{R}^+$ (or root mean square value, hereinafter RMS) of a given motion q_i,defined as:

$$\begin{aligned} \sigma_{q_i} &= \sqrt{m_{0_i}}, \\ m_{0_i} &= \int_{\mathbb{R}^+} S_{q_i} d\omega, \end{aligned} \tag{5}$$

where $m_{0,i} \in \mathbb{R}^+$ is the zero-order moment of the spectrum $S_{q,i}$.

Finally, the $\sigma_{q_i,k}$ values that synthesise the motion response to the k-th out of n_{waves} waves in the scatter can be weighted on the respective probability of occurrence of each sea states to obtain an overall RMS value (σ_{q_i}), summarising each motion response to the scatter for a specific floater.

In the top two plots in Figure 8 parametric curves for heave and pitch RMS values against the aspect ratio of the floater for different radii, are represented. Furthermore, in the bottom-side figure, costs parametric curves are exposed.

For increasing aspect ratio, *i.e.* for more slender cylindrical columns, it can be appreciated that both heave and pitch RMS values decrease. Similar behaviour is observed for increasing radii. On the other hand, cost increases with both aspect ratio and radius.

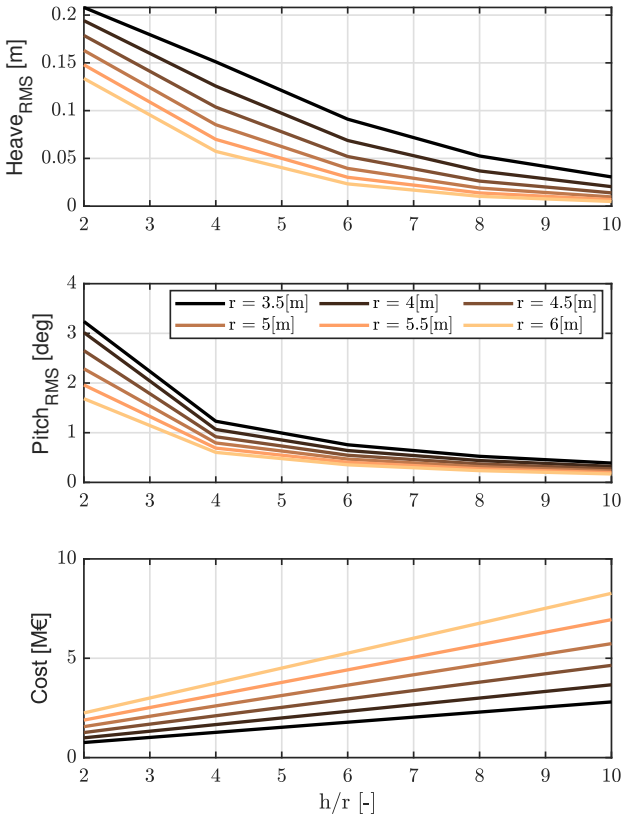

Figure 8: Results from the sensitivity analysis: heave RMS, pitch RMS, and cost against aspect ratio for different radii of the cylinder.

From the middle plot, looking at pitch RMS values, we can infer that is not too beneficial to design with aspect ratio larger than 4. In fact, once fixed a 3.5 m radius, shifting from aspect ratio 2 to 4 yields an attenuation of 62%, whilst shifting from 2 to 6 only increases the attenuation by about 15%. Conversely, the cost in the case $h/r = 6$ increases by 134% (with respect to $h/r = 2$), whilst in the case $h/r = 4$ only by 68%. In other words, for a further 15% attenuation in the pitch response, there is a 68% additional increase in costs. Similar reasoning can be applied, although less evidently, to other radii.

This behaviour is not however observed in the heave response, as we have a less steep decrease of the RMS value of the response with the aspect ratio. Nevertheless, when analysing the parametric curves for aspect ratios smaller than 6, one can notice a different shape depending on the value of the radius. For smaller radii, the curve is closer to a straight line: fixed a radius of 3.5 m, shifting aspect ratio 2 to 4 yields a first attenuation of 27.4%, and further shift to aspect ratio 6 yields a further 28.9% (with respect to the value for aspect ratio 2). When we fix a larger radius, *i.e.* for $r = 5$ m, we observe an attenuation of 47.7% after a change in aspect ratio from 2 to 4, and a further 31.5% attenuation after shifting from aspect ratio 4 to 6.

5 CONCLUSION AND FURTHER WORK

In this study, a preliminary investigation of the floating offshore deployment of AWESs is presented. We begin by providing an overview of existing floater concepts for traditional offshore wind energy systems, followed by a description of the key features of AWESs. Based on this analysis, we outlined that, driven by a cost effectiveness logic, a spar-like floating concept tailored to the requirements of AWES technology can be proposed, leveraging its unique opportunities while addressing its challenges.

Furthermore, a sensitivity study on the technology identified is conducted, providing, by leveraging a simplified description, insights into how geometrical properties, *i.e.* the radius and aspect ratio of the floater, influence its response. To evaluate the response a representative set of wave conditions are adopted, analysing Pantelleria's scatter as installation site.

The results indicate that adopting a height to radius radio $h/r = 4$ is advantageous for attenuating pitch response while also facilitating the design of a cost-efficient platform. However, if there are constraints on heave motion, a more slender floater may be necessary to mitigate this response, albeit at a significant increase in cost.

While this study results to be a preliminary assessment for the design of the floater for the support of an AWES in deep water, we believe that the non-mutual influence assumption of the floater and kite dynamics should be further investigated and verified under a larger set of conditions.

It is important to note that the current study does not consider the influence of the mooring system on the device dynamics. In fact, the mooring system will mitigate both heave and pitch responses of the floating platform, besides ensuring the station-keeping of the device in the surge and sway directions.

To address the presented limitations future work will include coupling of kite and mooring system dynamics in our model, aiming towards a more representative design of the floating offshore AWES.

REFERENCES

Ahrens, U., M. Diehl, & R. Schmehl (2013). *Airborne Wind Energy*. Springer Berlin, Heidelberg.

Cherubini, A., G. Moretti, & M. Fontana (2018). *Dynamic Modeling of Floating Offshore Airborne Wind Energy Converters*, pp. 137–163. Singapore: Springer Singapore.

Cherubini, A., A. Papini, R. Vertechy, & M. Fontana (2015). Airborne Wind Energy Systems: A review of the technologies. *Renewable and Sustainable Energy Reviews 51*, 1461–1476.

Cherubini, A., R. Vertechy, & M. Fontana (2016). Simplified model of offshore airborne wind energy converters. *Renewable energy 88*, 465–473.

Edwards, E. C., A. Holcombe, S. Brown, E. Ransley, M. Hann, & D. Greaves (2024). Trends in floating offshore wind platforms: A review of early-stage devices. *Renewable and Sustainable Energy Reviews 193*, 114271.

Erhard, M. & H. Strauch (2013). Control of towing kites for seagoing vessels. *IEEE Transactions on Control Systems Technology 21*(5), 1629–1640.

Erhard, M. & H. Strauch (2018, 04). Automatic control of pumping cycles for the skysails prototype in airborne wind energy. *Green Energy and Technology*, 189–213.

Fagiano, L. & M. Milanese (2012). Airborne Wind Energy: An overview. In *2012 American Control Conference (ACC)*, pp. 3132–3143.

Fagiano, L., M. Quack, F. Bauer, L. Carnel, & E. Oland (2022, 05). Autonomous airborne wind energy systems: Accomplishments and challenges. *Annual Review of Control, Robotics, and Autonomous Systems 5*.

Fritz, F. (2013, 10). Application of an automated kite system for ship propulsion and power generation. *Green Energy and Technology*, 359–372.

Ghigo, A., L. Cottura, R. Caradonna, G. Bracco, & G. Mattiazzo (2020). Platform optimization and cost analysis in a floating offshore wind farm. *Journal of Marine Science and Engineering 8*(11).

Jiang, Z. (2021). Installation of offshore wind turbines: A technical review. *Renewable and Sustainable Energy Reviews 139*, 110576.

Journée, J. & W. Massie (2000). *Offshore Hydromechanics*. TU Delft.

KitePower. https://thekitepower.com/the-falcon/ .

Loyd, M. L. (1980). Crosswind kite power (for large-scale wind power production). *Journal of Energy 4*(3), 106–111.

Ogilvie, T. (1964). Toward the understanding and prediction of ship motions. *Technische Hogeschool Delft: Delft, The Netherlands*.

Robertson, A., J. Jonkman, M. Masciola, H. Song, A. Goupee, A. Coulling, & C. Luan (2014, 9). Definition of the Semisubmersible Floating System for Phase II of OC4.

Saipem S.p.A. (2022). Hexafloat: lightweight pendulum floater for deep water and very large offshore wind turbines. Technical report.

SkySails Power. https://skysails-power.com/onshore-unit-pn-14/.

Trombini, S., E. Pasta, & L. Fagiano (2024). On the kite-platform interactions in offshore airborne wind energy systems: Frequency analysis and control approach. *European Journal of Control*, 101065.

van der Vlugt, R., J. Peschel, & R. Schmehl (2013, 09). Design and experimental characterization of a pumping kite power system. *Green Energy and Technology*, 403–425.